J Biol Inorg Chem (2002) 7: 146–156
DOI 10.1007/s007750100282

ORIGINAL ARTICLE

**Joris Messens · José C. Martins · Elke Brosens
KarolienVan Belle · Doris M. Jacobs · Rudolph Willem
Lode Wyns**

Kinetics and active site dynamics of *Staphylococcus aureus* arsenate reductase

Received: 15 March 2001 / Accepted: 2 June 2001 / Published online: 24 July 2001

Abstract Arsenate reductase (ArsC) encoded by *Staphylococcus aureus* arsenic-resistance plasmid pI258 reduces intracellular arsenate(V) to the more toxic arsenite(III), which is subsequently extruded from the cell. It couples to thioredoxin, thioredoxin reductase and NADPH to be enzymatically active. ArsC is extremely sensitive to oxidative inactivation, has a very dynamic character hampering resonance assignments in NMR and produces peculiar biphasic Michaelis-Menten curves with two V_{max} plateaus. In this study, methods to control ArsC oxidation during purification have been optimized. Next, application of Selwyn's test of enzyme inactivation was applied to progress curves and reveals that the addition of tetrahedral oxyanions (50 mM sulfate, phosphate or perchlorate) allows the control of ArsC stability and essentially eliminates the biphasic character of the Michaelis-Menten curves. Finally, ^{1}H-^{15}N HSQC NMR spectroscopy was used to establish that these oxyanions, including the arsenate substrate, exert their stabilizing effect on ArsC through binding with residues located within a C-X_5-R sequence motif, characteristic for phosphotyrosine phosphatases. In view of this need for a tetrahedral oxyanion to structure its substrate binding site in its active conformation, a reappraisal of basic kinetic parameters of ArsC was necessary. Under these new conditions and in contrast to previous observations, ArsC has a high substrate specificity, as only arsenate could be reduced ($K_m = 68$ μM, $k_{cat}/K_m = 5.2\times10^4$ M^{-1} s^{-1}), while its product, arsenite, was identified as a mixed inhibitor ($K^*_{iu} = 534$ μM, $K^*_{ic} = 377$ μM).

Keywords Arsenate reductase · Kinetics · NMR spectroscopy · Redox enzyme · Selwyn test

Abbreviations *AEBSF*: 4-(2-aminoethyl)benzenesulfonyl fluoride hydrochloride · *DSS*: sodium 4,4-dimethylsilapentanesulfonate · *DTT*: dithiothreitol · *HSQC*: heteronuclear single quantum correlation spectroscopy · *INEPT*: insensitive nuclei enhanced by polarization transfer · *MM*: Michaelis-Menten · *RPC*: reverse phase chromatography · *TPPI*: time proportional phase incrementation · *TR*: thioredoxin reductase · *Trx*: thioredoxin

J. Messens (✉) · J.C. Martins · E. Brosens · K. Van Belle
L. Wyns
Dienst Ultrastructuur, Vlaams interuniversitair
Instituut voor Biotechnologie (VIB),
Vrije Universiteit Brussel, Paardenstraat 65,
1640 Sint-Genesius-Rode, Belgium
E-mail: jmessens@vub.ac.be
Tel.: +32-2-3590249
Fax: +32-2-3590289

J.C. Martins · D.M. Jacobs · R. Willem
High resolution NMR Centre,
Vrije Universiteit Brussel, Pleinlaan 2,
1050 Brussels, Belgium

Introduction

Oxyanions of arsenic and antimony that enter cells via transporters for other compounds are highly toxic, especially in oxidation state +III [1]. In *Staphylococcus aureus*, arsenate (AsO_4^{3-}) is taken up by the phosphate transport systems [2]. Once inside, resistance to arsenite (AsO_2^-) and antimonite (SbO_2^-) results from active extrusion of the toxic +III oxyanions [3, 4, 5]. Arsenate resistance requires an additional protein (ArsC) which reduces intracellular arsenate to arsenite [6], the form recognized by the efflux system. Arsenic and antimony resistance on *ars* operons can be found on plasmids and chromosomes [7]. In *S. aureus*, three genes termed *arsRBC* have been identified on plasmid pI258 [8, 9]. ArsR is an As(III)/Sb(III)-responsive transcriptional repressor [9]. ArsB is a secondary transporter that catalyses efflux of the arsenite anion from cells [5]. The 131-residue ArsC protein (M_w 14,812.7) encoded by the *arsC* gene shares only 12% sequence identity with ArsC found on plasmid R773 in *E. coli* [10], and no sequence identity with Acr2p of chromosome XVI from *S. cerevisiae* [11]. Nevertheless, these three arsenate reductases from different biological

sources do share a Cys-X_n-Arg consensus sequence, which is also the characteristic catalytic sequence motif found in phosphotyrosine phosphatases (PTPases) [12, 13]. In particular, ArsC from *S. aureus* shares 20–30% sequence identity with members of the family of "low M_r protein tyrosine phosphatases". In the latter, the active site sequence motif is located near the N-terminus, and features a conserved V/I-C-X-G-N-X-C-R-S sequence, referred to as the P-loop [14, 15]. This sequence motif corresponds exactly to the one found in ArsC from *S. aureus*. Since ArsC proteins and phosphatases both have oxyanions as substrates, this might indicate similarities in protein oxyanion binding.

In vitro, ArsC from *S. aureus* pI258 requires coupling to thioredoxin (Trx), thioredoxin reductase (TR) and NADPH in order to be enzymatically active (Fig. 1) [10, 16]. *S. aureus* ArsC has four cysteinyl residues, Cys10, 15, 82 and 89. Cys10, 82 and 89 are essential for enzymatic activity and the reduction of arsenate to arsenite results in the formation of an intramolecular Cys82-Cys89 disulfide bond. In contrast, ArsC from *E. coli* R773 and Acr2p from *S. cerevisiae* both have only one essential cysteine located within the P-loop sequence motif. This cysteine residue forms a mixed disulfide with glutathione after arsenate reduction and is regenerated through the action of glutaredoxin [11, 17]. Thus, despite the conserved sequence motif, these observations make *S. aureus* ArsC from pI258 a different redox enzyme with another catalytic mechanism [10]. As such, it is the first and best studied member of a new family of oxyanion reductases that might include, based on their sequence identity, ArsC from *S. xylosus* (94%), *Sinorhizobium* sp. As4 (70%), *B. subtilis* (64%) and *B. halodurans* (61%).

The optimization of the assay conditions in a complete *S. aureus* based system (Trx, TR) and a thorough kinetic study are reported. To guarantee a fully redox-active enzyme in all our assays, adaptation of the previously published purification protocol [10, 18] proved necessary. The stability of ArsC and its dependence on oxyanions through the assay was investigated using Selwyn's test of enzyme inactivation [19]. In addition, the structural influence of these oxyanions on ArsC was studied with ^{1}H-^{15}N heteronuclear NMR.

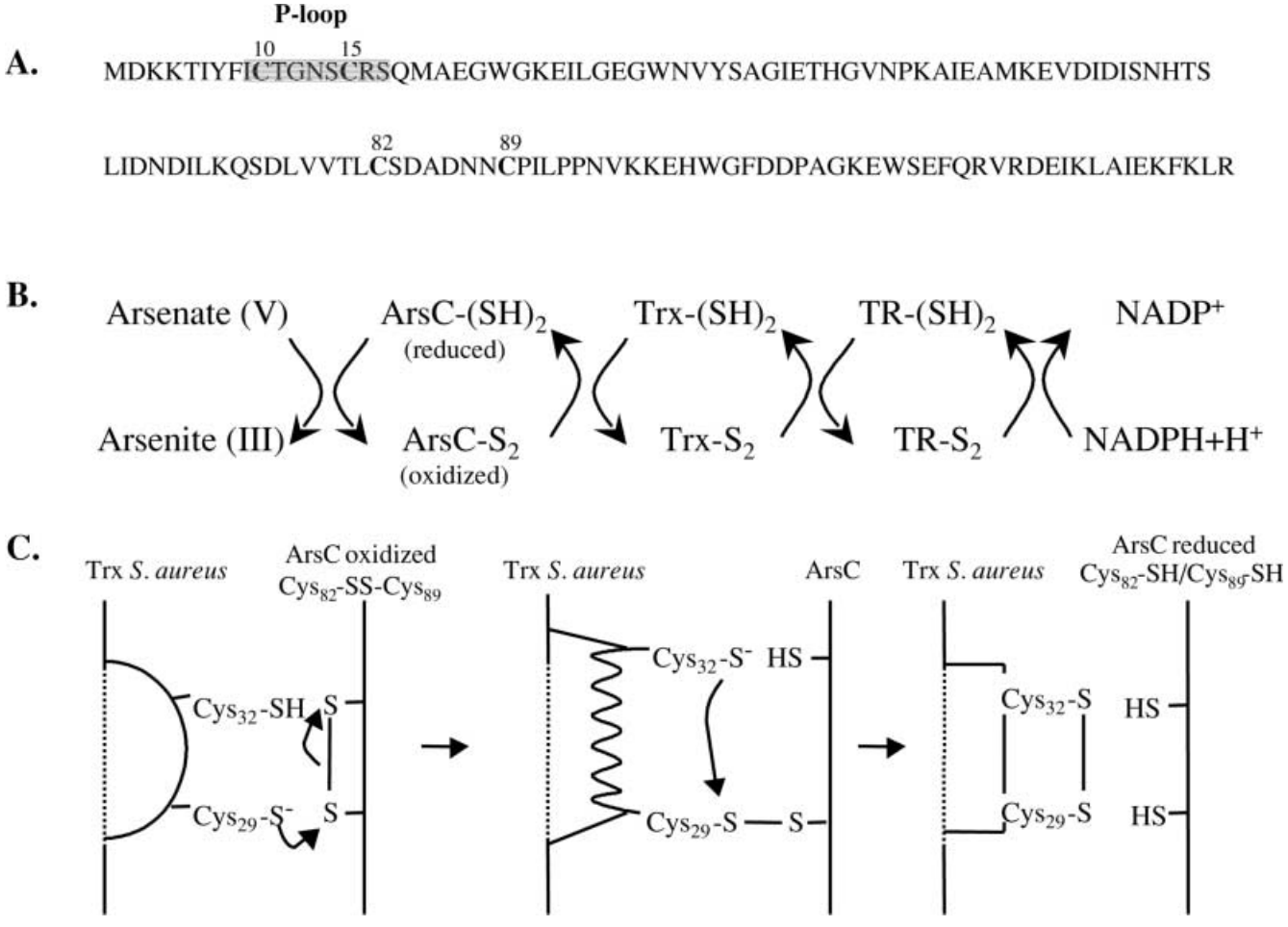

Fig. 1A–C The coupled enzymatic reaction of *S. aureus* ArsC. **A** Sequence of ArsC wild-type in one-letter code with the cysteines in *boldface* (*sequence position on top*). The position of the P-loop is indicated with a *grey box*. **B** The coupled enzymatic cascade from arsenate to the formation of NADP. **C** Detail of the regeneration of oxidized ArsC by *S. aureus* Trx

Materials and methods

Expression and purification of arsenate reductase

The *arsC* wild-type gene from *S. aureus* was cloned into a pET-11a vector (Stratagene, La Jolla, Calif.) by introducing restriction sites *Nde*I and *Bam*HI with PCR. The *E. coli* strain BL21 (DE3) was transformed with the pET-11a *arsC* wild-type plasmid [20] and was grown for 5 h at 37 °C in Terrific broth (TB) with 100 μg/mL ampicillin. Induction at a cell density of $OD_{600} = 2$ was carried out overnight with 1 mM IPTG at 28 °C. Cells were harvested ($OD_{600} = 16$), disrupted and purified as described before [10], except for the following changes. As cell-disruption-buffer, 100 mM Tris/HCl (pH 8.0) with 50 mM NaCl, 20 mM 2-mercaptoethanol, 0.1 mM EDTA, 0.1 mg/mL 4-(2-aminoethyl)benzenesulfonyl fluoride hydrochloride (AEBSF) and 1 μg/mL leupeptine was used. In all other buffers, 1 mM dithiothreitol (DTT) was added and in the gel filtration buffer an extra 50 mM K_2SO_4 was added. All buffers were argon flushed for several minutes prior to use and all concentration steps were performed on Vivaspin 5 kDa cut-off concentrators (Vivascience, Lincoln, UK). After the gel filtration run, ArsC was concentrated, flash frozen in liquid nitrogen and stored at –20 °C. Protein yield was approximately 16 mg/L culture.

Prior to use in the kinetic assays, the sample was reduced with 10 mM DTT during 30 min at room temperature and injected on a Jupiter C18 (10 μm, 300 Å, 10×250 mm) reverse phase column (Phenomenex, St. Torrance, Calif.) operated on an Äkta-explorer [Amersham Pharmacia Biotech (APB), Uppsala, Sweden]. The column was equilibrated with 20 mM Tris/HCl (pH 8.0) 10 mM K_2SO_4, 1 mM DTT, 15% acetonitrile (argon flushed) and eluted with a 20-column volume gradient to 45% acetonitrile in the same buffer at 8 mL/min. The different peaks were collected separately and dialyzed against 20 mM Tris (pH 8.0), 50 mM K_2SO_4, 0.1 mM EDTA, 1 mM DTT to remove acetonitrile.

The ArsC C15A mutant was constructed and purified as described [10] followed by the extra reverse phase purification step on Jupiter C18 mentioned above.

Expression/purification of thioredoxin and thioredoxin reductase from *S. aureus*

The *trxA* and *trxB* genes from *S. aureus* were cloned into the *Nde*I and *Bam*HI sites of pET-14b (Novagen, Madison, Wis.).

For thioredoxin from S. aureus

The *E. coli* strain BL21 (DE3) was transformed with the pET-14b *trxA* and grown overnight at 37 °C in a Luria-Bertani broth (LB) preculture with 100 μg/mL ampicillin. The culture was diluted 100-fold into TB with ampicillin and further grown at 37 °C. Induction was started at a cell density of $OD_{600} = 2$ with 1 mM IPTG and carried out overnight at 28 °C. Cultures were harvested at a cell density of $OD_{600} = 20$ and suspended in 20 mM Tris/HCl (pH 7.9), 5 mM imidazole, 1 M NaCl, 1 mM DTT, 0.1 mg/mL AEBSF and 1 μg/mL leupeptin (argon flushed) to a final cell density of approximately $OD_{600} = 200$. Following French press disruption, 50 μg DNase I/mL (EC 3.1.21.1; Sigma, St. Louis, Mo.) and 20 mM $MgCl_2$ were added to the lysate. After 30 min at room temperature, cell debris were removed by centrifugation for 30 min at 12,000×*g* at 4 °C, fresh 1 mM DTT was added and the lysate was filtered. The lysate was purified at 10 mL/min on a 3 mL Ni^{2+}-NTA Superflow (Qiagen, Valencia, Calif.) immobilized-metal-affinity column equilibrated with 20 mM Tris/HCl (pH 7.9), 1 M NaCl, 1 mM DTT and eluted with a linear gradient to 1 M imidazole in the same buffer. The proteins under the main elution peak were concentrated, fresh 1 mM DTT was added and further purified on a Superdex75 PG (16/90) gel filtration column (APB) in 20 mM Tris/HCl (pH 8.0), 150 mM NaCl, 1 mM DTT. Under these conditions a final Trx yield of approximately 11 mg/L culture was obtained. Purity was checked on SDS-PAGE and Trx was stored frozen. All buffers were argon flushed and runs were performed on a FPLC (APB) at room temperature.

For thioredoxin reductase from S. aureus

The *E. coli* strain BL21 (DE3) was transformed with the pET-14b *trxB*. Cell growth conditions were as described for thioredoxin, except that the culture was induced at a cell density of $OD_{600} = 0.6$ with 0.4 mM IPTG. Culture was harvested at a cell density of $OD_{600} = 17$. A similar purification scheme as for Trx was followed with an extra step on a 10 mL 2′,5′-ADP-Sepharose 4B (APB) column equilibrated with 20 mM Tris (pH 7.6). TR was eluted with a step gradient at 0.7 M NaCl in the same buffer. This extra purification step gave the required purity, as checked on SDS-PAGE. The proteins under the peak were concentrated to 5 mg/mL and stored as a 80% ammonium sulfate precipitate at 4 °C. The final TR yield was 32 mg/L culture.

NMR spectroscopy

Samples for NMR spectroscopy consisted of 1.8 mM solutions of ^{15}N-labelled ArsC obtained as described elsewhere [21], and in 50 mM phosphate buffer (pH 6.7) to which 0.1 mM EDTA, 1 mM DTT and 5% D_2O were added unless mentioned otherwise. Changes in salt contents were performed either by direct addition from a concentrated stock solution or by dialysis using a Slide-A-Lyzer with 3.5 kDa cut-off against a buffer with appropriate composition. Samples were transferred to Shigemi tubes and all measurements were performed at 298 K on a Bruker AMX500 spectrometer upgraded with digital lock and SGI O2 computer and operating at 500.13 and 50.68 MHz for ^1H and ^{15}N, respectively. The 2D ^1H-^{15}N heteronuclear single quantum correlation spectroscopy (HSQC) spectra [22] were recorded with gradients for artifact suppression and water-flip back pulses to avoid saturation of the amide resonances [23]. Sodium 4,4-dimethylsilapentanesulfonate (DSS) was used as internal reference for the ^1H and ^{15}N chemical shifts [24]. WATERGATE [25] applied during the final insensitive nuclei enhanced by polarization transfer (INEPT) was used for optimal suppression of the water resonance [23], with ^{15}N decoupling during acquisition using WALTZ16. All 2D spectra were recorded with a spectral width of 14.08 ppm and 32 ppm in the ^1H and ^{15}N dimension, respectively, using States-time proportional phase incrementation (TPPI) [26]. The total recycling delay was 1.1 s; 8–32 scans, 1024 data points each, were recorded for a total of 256 t_1 increments. Processing consisted of one order of linear prediction along F_1, multiplication with a $\pi/2$-shifted squared sinebell in F_2 and F_1 and zero filling to yield a 1K×1K complex data matrix after Fourier transformation, all using the Felix 98.0 software package (MSI, San Diego, Calif.).

SDS-PAGE analysis

ArsC was analyzed on pre-cast 10% Bis-Tris NuPage SDS-PAGE [27] with a SDS MES running buffer in a Xcell II mini-Cell as recommended by the manufacturer (Novex, San Diego, Calif.).

Mass spectrometry

Electrospray mass spectrometry was carried out with a Quattro II quadrupole mass spectrometer (Micromass, Manchester, UK) having a m/z range of 4000, as described previously [18].

Assay of arsenate reductase activity

Trx was defrosted and reduced with 20 mM DTT at room temperature for 30 min and subsequently dialyzed in a Slide-A-Lyzer 3.5 K (Pierce, Rockford, Ill.) against 50 mM Tris/HCl (pH 8.0),

100 mM NaCl, 0.1 mM EDTA. A sample of the TR ammonium sulfate stock was pelleted, dissolved and dialyzed against the same buffer. NADPH (Sigma, St Louis, Mo.) was dissolved in water to a stock concentration of 50 mM and stored at 4 °C. Arsenate ($Na_2HAsO_4.7H_2O$, Sigma) was freshly dissolved in water at 1 M for making dilution series. The assay buffer was 50 mM Tris (pH 8.0), 50 mM K_2SO_4 and 0.1 mM EDTA (argon flushed). Just before use, ArsC was dialyzed against the assay buffer to remove DTT. The final assay mixture was prepared by diluting all components except the substrate in the assay buffer to obtain 100 nM ArsC, 10 μM Trx, 2 μM TR and 500 μM NADPH (=component mixture), taking into account the subsequent addition of substrate, unless specifically mentioned in the results. Protein concentrations were determined from the calculated specific extinction coefficient at 280 nm [28]. The component mixture was incubated without substrate at 37 °C in a 96-well plate (PolySorb, Nunc, Denmark) (180 μL/well) in a SPECTRAmax340PC (Molecular Devices, Sunnyvale, Calif.) for 5 min. The assay was started by the addition of dilution series of substrate (20 μL/well) to obtain a final volume of 200 μL/well. The arsenate reduction coupled to NADPH oxidation ($\Delta\varepsilon_{340} = 6220\ M^{-1}\ cm^{-1}$) was measured by following the decrease in absorption at 340 nm. The path length was measured after each run for each well with the PathCheck Sensor of the system and was used for k_{cat} calculations. Initial rates were calculated with SPECTRAmaxPro (Molecular Devices). Kinetic plots were made with Origin 5.0 (Microsoft) using the Michaelis-Menten (MM) expression and/or the mixed inhibition expression to calculate V_{max} and k_{cat} values, K_{iu} and K_{ic}. K_{iu} and K_{ic} were also determined with the median estimates from the direct linear plots calculated with Matlab (The Math Works, Mass.). For the Selwyn test of enzyme inactivation, different enzyme concentrations (25, 50, 100 and 200 nM) were used in the presence of different oxyanions (50 mM K_2HPO_4, 50 mM K_2SO_4, 50 mM $NaClO_4$ and 50 mM KNO_3) and different KCl concentrations (50, 150 and 500 mM). For the Selwyn test in the presence of 50 mM Na_2HAsO_4, the reaction was started by adding the (Trx, TR, NADPH) mixture to different concentrations of ArsC incubated with 50 mM Na_2HAsO_4.

For the substrate specificity assays, phosphate (K_2HPO_4), sulfate (K_2SO_4), nitrate (KNO_3), tellurate (K_2TeO_4, Aldrich), selenate (K_2SeO_4, Aldrich), selenite (K_2SeO_3, Aldrich) and antimonate ($KSbO_3$, Fluka) were tested next to arsenate. For the inhibition assays, together with the mentioned component mixture, dilution series of several inhibitors were incubated for 5 min at 37 °C before the reaction was started by adding arsenate. The following inhibitors in different dilution series were tested: arsenite ($NaAsO_2$, Sigma), tellurite (K_2TeO_3, Sigma), antimonite [$K(SbO)C_4H_4O_6{\cdot}0.5H_2O$, Fluka], antimonate ($KSbO_3$, Fluka) and tellurate ($K_2TeO_4$, Aldrich). For the pH study, 50 mM Tris or 50 mM Bis-Tris was used in the assay buffer to cover the whole pH range (from pH 6.2 to 8.8) with enough buffer capacity. A kinetic plot was measured every 0.2 pH unit and each was used to calculate k_{cat} and K_m values in this pH range.

Results

Control of the oxidative sensitivity of ArsC

Kinetic properties of ArsC had already been measured in different kinetic studies under different assay conditions [10, 16]. In our experience, however, k_{cat} values with otherwise identical assay conditions were difficult to reproduce and varied with the age as well as with the homogeneity of samples produced from different batches. Therefore, further optimization of the purification procedure of this highly oxidation sensitive redox-enzyme was undertaken.

Previously, ArsC has been purified with an ammonium sulfate cut, followed by a capture step on a hydrophobic interaction matrix, an intermediate anion-exchange purification step and a polishing step on a size-exclusion column [10, 18]. The most important improvement in the purification method proposed here consists of an increase in the concentration of reductant and the flushing of all buffers used with argon, in order to avoid any possible irreversible oxidation and to ensure the thiol state for all four cysteines. To stabilize ArsC during purification, K_2SO_4 was added to all buffers (explanation below), except for the anion-exchange buffer, where low conductivity is necessary to bind to the column [18]. Last but not least, the addition of a reverse phase separation step at pH 8.0 on an inert silica reverse phase chromatography (RPC) column resulted in the separation of fractions (P1, P2, P3) of ArsC with different catalytic properties (Fig. 2). The P1 and P2 fractions contained oxidized methionines/cysteines (+16 Da) and formylated (+28 Da) ArsC forms, as deduced from mass spectrometry. The fraction P3 contained a single ArsC species with a mass of 14,812 Da, which is consistent with the calculated mass of reduced ArsC. P3 corresponds to the lower single band on SDS-PAGE [27] with an aberrant migration position (<14.4 kDa) and shows the highest activity when compared to the other ArsC species. With this extra purification step, therefore, pure ArsC is now available for characterization.

Stability of ArsC

A most unusual and peculiar observation with this enzyme already reported by Ji et al. [16], and confirmed here, is that of a kinetic curve, rate versus substrate concentration, exhibiting two plateaus (Fig. 3, circles). While one may associate this with two k_{cat} values differing by a factor of ca. 5 and with strongly different K_m values (factor of ca. 50), it provides little clues as to the physical basis for this biphasic behavior. Apparently, the enzyme becomes stabilized at higher concentrations of the arsenate substrate, possibly as a result of another ionic strength regime. To further investigate this unusual phenomenon and in view of its highly oxidation sensitive character, we have applied Selwyn's test of enzyme inactivation to ArsC [19].

Selwyn's test of enzyme inactivation

The stability of the enzymatic activity of ArsC was tested by evaluating the decrease in rate in progress curves under various assay conditions. If progress curves are obtained with various concentrations of ArsC but otherwise identical assay conditions, plots of formed product against an abscissa of time multiplied by enzyme concentration should be superimposable. If they are not, the rate depending on the enzyme concentration changes throughout the reaction and so the enzymati-

cally active ArsC concentration must be variable. To evaluate ionic strength effects, various concentrations of ArsC (25, 50, 100, 200 nM) were analyzed in the presence of KCl at different concentrations (50, 150 and 500 mM). The specificity of the stabilizing effect for the nature of the anion was tested in the presence of several oxyanions (KNO_3, K_2SO_4, K_2HPO_4, $NaClO_4$ and Na_2HAsO_4) at 50 mM, pH 8.0 (Fig. 4). It turned out that KCl and KNO_3 were not stabilizing ArsC as four different progress curves were observed each time. The tetrahedral oxyanions phosphate, sulfate and perchlorate, however, were found to stabilize ArsC, starting from 50 nM ArsC. As can be observed from Fig. 4, the best stabilizing oxyanion was its substrate arsenate, for which all points fell on the same curve over the whole range of ArsC concentrations tested.

NMR study on the influence of oxyanions on the conformation of ArsC

NMR spectroscopy was used to investigate whether the stabilizing effect was due to specific interactions of the oxyanions with ArsC. This was made possible by the recently completed backbone resonance assignment of ^{15}N-labeled ArsC [21]. A remarkable observation throughout this assignment was the absence of the ^{1}H-^{15}N correlations corresponding to the amide group of residues Thr11 to Ser17 (P-loop) in the HSQC spectrum of the reduced ArsC, even in 50 mM phosphate buffer solution (Fig. 5A). Such absence might result from fast chemical exchange of the labile amide protons with the solvent, especially when these are solvent exposed. Alternatively, this part of the structure could also experience some conformational flexibility, leading to exchange broadening of the NH correlations. After addition of 50 mM K_2SO_4 the missing correlations appear in the ^{1}H-^{15}N HSQC spectrum, indicating a dramatic effect of this tetrahedral oxyanion on the conformation and dynamics of the Cys10-X_5-Arg16 segment (Fig. 5B) and this irrespective of the redox state of ArsC. The effect of arsenate, the most stabilizing oxyanion identified from Selwyn's test, was also investigated. Upon addition of 50 mM arsenate to ArsC in phosphate buffer, only the singly oxidized form (Cys82-Cys89) was observed in the HSQC spectra, as arsenate in excess leads to complete oxidation within minutes of sample preparation. Also here, however, the addition of 50 mM arsenate leads to the appearance of the NH correlations of the Thr11-Ser17 segment, albeit at significantly different positions in the ^{1}H-^{15}N HSQC spectra, as compared with sulfate. This difference in peak positions was exploited to establish that the

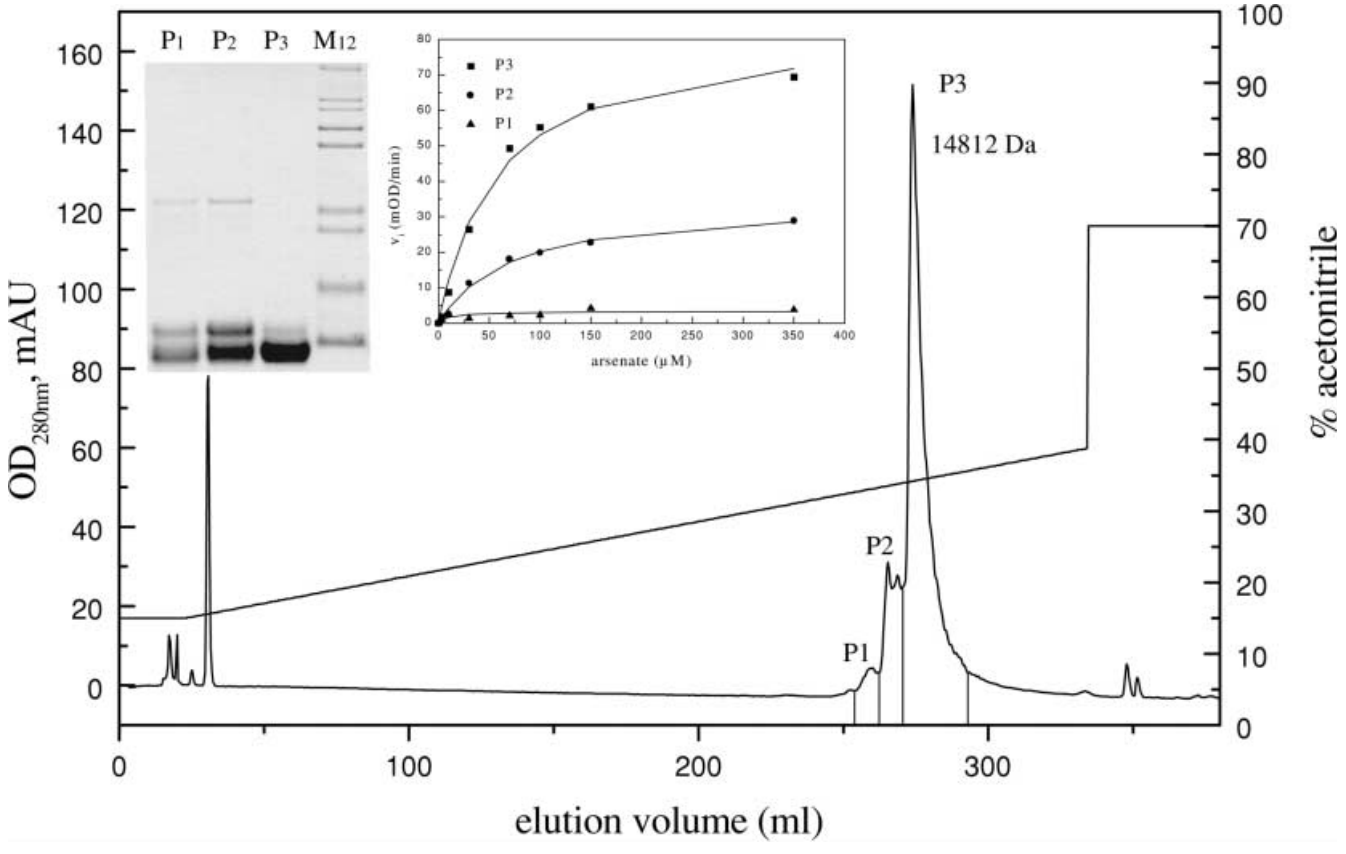

Fig. 2 Analysis of the fractions obtained after C18 RPC. Chromatographic elution profile at 280 nm of ArsC injected on a Jupiter C18 column at pH 8.0. Fractions were analyzed on SDS-PAGE next to the protein marker M12 (Novex) of 200, 116.3, 97.4, 66.3, 55.4, 36.5, 31, 21.5 and 14.4 kDa and in the arsenate reductase assay. The kinetic plots of the initial velocity (v_i) versus substrate concentrations are shown for 100 nM of each fraction

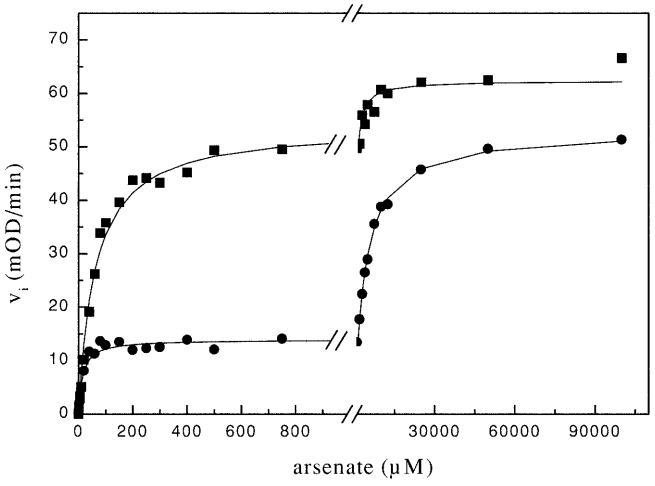

Fig. 3 Michaelis-Menten kinetic plots of ArsC. Initial velocity (v_i) versus arsenate concentration measured in 50 mM Tris (pH 8.0), 150 mM KCl, 0.1 mM EDTA (argon flushed) (*circles*) and in 50 mM Tris (pH 8.0), 50 mM K_2SO_4, 0.1 mM EDTA (argon flushed) (*squares*)

oxyanions interact with ArsC through direct binding. Using ^{1}H-^{15}N HSQC, the dialysis of the 50 mM arsenate sample against a buffer solution containing 50 mM sulfate was monitored by ^{1}H-^{15}N HSQC (Fig. 5C). After only 3 h of dialysis, the resonances of oxidized ArsC in the presence of arsenate are seen to co-exist with those of oxidized ArsC in the presence of sulfate, indicating mutual competition of arsenate and sulfate for the same Cys10-X_5-Arg16 site (Fig. 5D). After another 3 h of dialysis, only the spectrum of oxidized ArsC bound to sulfate remained visible (Fig. 5E). The gradual replacement of arsenate by sulfate significantly perturbs the cross peaks from Cys10-X_5-Arg16 and the residues immediately surrounding them, which demonstrates the existence of this P-loop as the oxyanion binding site in ArsC.

Biphasic character of the MM curve

The stabilizing effect of oxyanions through interaction with the Cys10-X_5-Arg16 segment can now be used to explain the two-step kinetic curve behavior of ArsC observed here and in earlier reports [10, 14] (Fig. 3, circles). The second, unexpected rise in the kinetic plot is due to the stabilizing effect of the tetrahedral oxyanion arsenate at millimolar concentrations, resulting in an apparent second k_{cat} value. At low arsenate concentrations, only a fraction of ArsC is available in

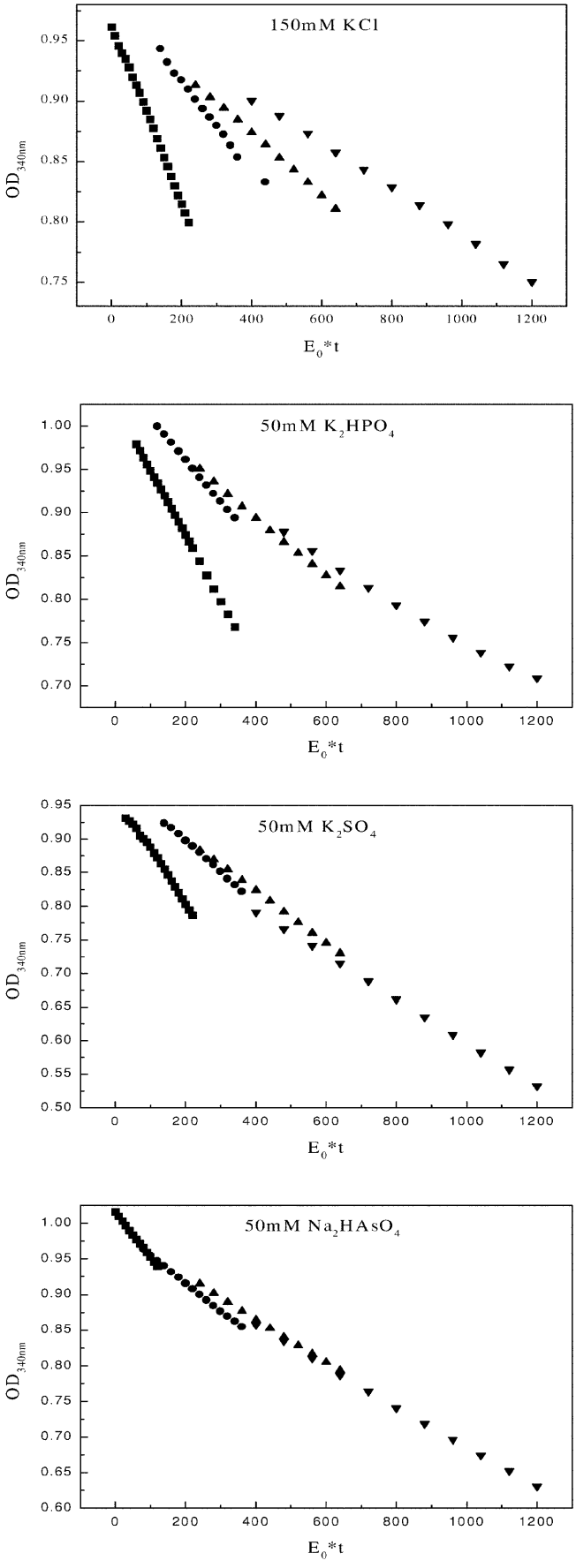

Fig. 4 Stability of ArsC during the enzymatic assay. Selwyn's test of enzyme inactivation: progress curves plotted against initial enzyme concentration (E_0) multiplied by time (t) at different enzyme concentrations (*squares* = 25 nM, *circles* = 50 nM, *triangles* = 100 nM, *reverse triangles* = 200 nM). The effect of KCl compared with tetrahedral oxyanions is shown

its enzymatically active state, which results in an apparent low k_{cat} value. Since the best stabilizing agent of ArsC is its substrate at 50 mM concentration, it is obviously impossible to measure the MM curve with values for low arsenate concentrations with arsenate as the sole oxyanion. For the enzyme assays as a function of arsenate concentration in the low arsenate concentration range, phosphate (50 mM), sulfate (50 mM) and perchlorate (50 mM) are non-substrate oxyanions stabilizing the redox enzyme, and the same k_{cat}/K_m values result from analyses in their presence. Thus, by using 50 mM K_2SO_4 instead of 150 mM KCl, at the same ionic strength, the first rise in the MM curve was strongly enhanced (Fig. 3, squares). The second increase, which is now minor but still present, is probably due to the fact that arsenate is the better stabilizing oxyanion compared to sulfate, as was already visible from the Selwyn tests. As a result, all the assays were subsequently performed in the presence of 50 mM sulfate as stabilizing oxyanion.

Fig. 5A–E Panels showing selected regions of ^{1}H-^{15}N HSQC spectra of ArsC in solution, demonstrating the effect of phosphate, sulfate and arsenate on loop residues. Each residue in these spectra contributes to one single peak that originates from the backbone NH group. **A** Spectrum of reduced ArsC at 298 K recorded in a 50 mM phosphate buffer. **B** Same sample following dialysis to a 50 mM phosphate buffer containing 50 mM K_2SO_4. In both panels, the *inset* shows the spectral areas where Arg16 and Gln18 are observed. ^{1}H-^{15}N amide correlations of residues Thr11-Gly12-Asn13-Ser14-Cys15-Arg16-Ser17-Gln18 in the loop which appear in the presence of K_2SO_4 are labeled in **B**, while *circles* highlight their absence in **A**. Note the shift of the Gln18 ^{1}H-^{15}N correlation peak with respect to its position in the presence of K_2SO_4. **C–E** Details of spectra of oxidized ArsC at 298 K obtained after addition of 50 mM arsenate to a phosphate buffer solution of reduced ArsC (**C**) and following 3 h (**D**) and 6 h (**E**) of dialysis against a phosphate buffer containing 50 mM K_2SO_4. The *insert* shows the spectral area where Gln18 is observed. Cross-peaks from the same residue in the different oxyanion bound forms of ArsC are connected by *lines*

MM conditions for arsenate reductase activity

For ArsC, there is no convenient way to monitor the formation of arsenite directly. Therefore, the reaction is followed indirectly by observing the rate of NADP formation. The coupling enzymes in the cascade towards NADPH are thioredoxin and thioredoxin reductase, delivering reducing equivalents to the oxidized ArsC (Fig. 1). It is well known that while the active site cysteines of Trx are essential for protein reduction, the participation of the integral structure in the Trx-target recognition process modulates its efficiency in doing so [29]. Therefore, we used Trx and TR from *S. aureus* for the kinetic study of ArsC. Both were recombinantly overproduced in *E. coli* and purified to homogeneity on immobilized metal-affinity chromatography followed by gel filtration (see Material and methods). For the NADPH-dependent flavoprotein TR, an extra affinity chromatography step on 2′,5′-ADP-Sepharose was necessary to obtain the required degree of purity. The purity was checked on reduced SDS-PAGE.

The concentrations of Trx and TR have to be high so that their action is not rate limiting [30]. Otherwise, the progress curves will show a lag-phase and the use of initial rates for calculating kinetic plots will lead to false cooperativity. Kinetic plots were measured with varying Trx (0.2–10 μM) and TR concentrations (1–2 μM).

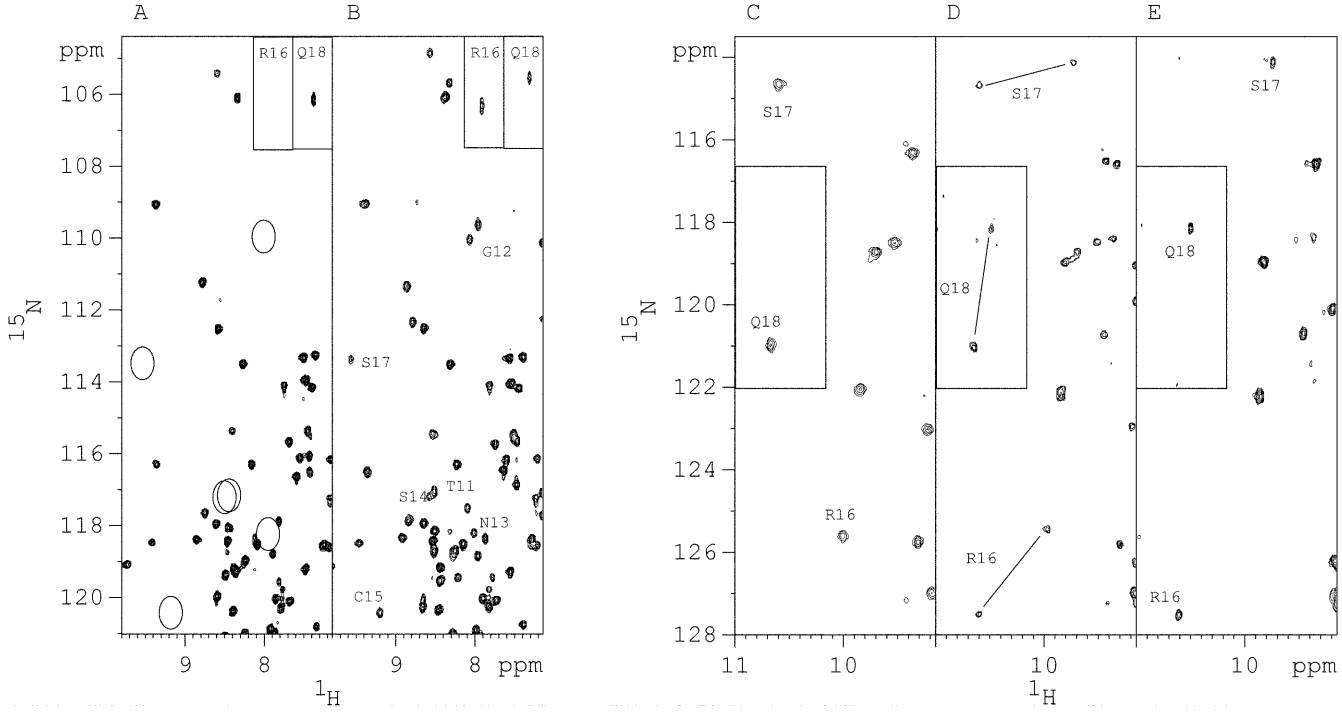

These TR concentrations in the assay were found to be sufficiently high and have a minimal effect on the observed V_{max} in the range 0.2–2 μM Trx. The Trx concentration was observed to be crucial in order to avoid false cooperativity. Especially at Trx concentrations lower than the K_m of Trx for TR ($K_m = 0.55$ μM; O. Uziel, unpublished results), extremely high Hill factors were obtained. The minimum Trx and TR concentrations required in order to obtain a rectangular hyperbolic MM expression are respectively 10 μM and 2 μM. Increasing these concentrations gave no further gain in V_{max}. Thus, concentrations of the various components in the coupled enzyme assay necessary to yield MM kinetics were found to be 100 nM ArsC, 10 μM Trx, 2 μM TR and 500 μM NADPH.

pH dependence of the kinetic parameters of ArsC

Between pH 6.5 and 8.5, kinetic plots with a Hill coefficient of 1 were measured for ArsC. Outside these pH boundaries, the Hill coefficients were higher than 1, which might be due to the instability of ArsC, Trx or TR. The k_{cat} and K_m data for nine MM kinetic plots obtained between pH 6.5 and 8.5 were measured. Changes of the slope in the plot $\log(k_{cat}/K_m)$ against pH reflect ionization of free, unbound enzyme or free substrate and resulted in apparent pK_{a1} and pK_{a2} values of approximately 7 and 8, respectively. A linear increase of k_{cat} was observed with increasing pH. The K_m was in the low 50–80 μM range up to pH 8.0 and steeply increased above pH 8.0 towards a maximum of 0.44 mM at pH 8.5. As such, the optimal pH for determining the kinetic properties of ArsC was pH 8.0, the pH where MM conditions were obeyed at the highest rate with a low K_m.

What is the significance of such a macroscopic observation? The pK_a values of arsenate are 2.24 (pK_{a1}), 6.96 (pK_{a2}) and 11.5 (pK_{a3}) [31]. The first apparent pK_a value might therefore reflect the pK_{a2} of the substrate, arsenate. This interpretation is in line with the absence of any changes in the ^{1}H-^{15}N HSQC spectrum of ArsC in the range pH 6.7–7.5 (data not shown). From pH 8.0 onwards, global changes in the protein spectrum prevent the attribution of pK_a shifts to specific residues. Therefore, it was impossible to use NMR to determine whether the second pK_a at pH 8.0 was linked to a microscopic pK_a value of a critical residue in the reductase reaction. However, the pronounced changes in the ^{1}H-^{15}N HSQC spectrum of ArsC above pH 8.0 suggest its kinetic behavior may be affected by a dramatic conformational change.

Substrate specificity

Kinetic measurements indicate that K_2SO_4, K_2HPO_4 and KNO_3 are no substrates for ArsC. Owing to the limited solubility of potassium antimonate and tellurate, it was not possible to assay concentrations higher than respectively 10 mM and 1 mM and at this concentration no NADPH oxidation was observed. In this coupled enzyme assay it was also impossible to generate kinetic data with selenate and selenite. Both oxyanions give extremely high background by activating the coupled enzyme assay in the absence of ArsC. Under the optimized assay conditions, only arsenate was found to be a substrate for ArsC wild-type, displaying $K_m = 68$ μM, $k_{cat} = 215$ min^{-1} and $k_{cat}/K_m = 5.2\times10^4$ M^{-1} s^{-1}. Mutations of Cys10, 82 and 89 (Fig. 1) led to redox-inactive enzymes and for the only active Cys mutant of ArsC [10], ArsC C15A, $K_m = 192$ μM, $k_{cat} = 248$ min^{-1} and $k_{cat}/K_m = 2.15\times10^4$ M^{-1} s^{-1} were measured (Fig. 6).

Inhibitors of ArsC

The product of arsenate reductase, arsenite, behaves as an inhibitor. In plots of initial velocity (v_i) against inhibitor concentration (i) at various substrate concentrations, data were fitted to the hyperbolic equation for mixed inhibition:

$$v_i = \frac{dp}{dt} = \frac{Va}{K_m(1 + i/K_{ic}) + a(1 + i/K_{iu})} \quad (1)$$

where a is the substrate concentration, resulting in a mean competitive inhibitor constant $K_{ic} = 434$ μM and a mean uncompetitive inhibitor constant $K_{iu} = 563$ μM. Via linear Dixon [32] and Cornish-Bowden plots [33] ($1/v_i$ plotted against i and a/v_i plotted against i at various concentrations of a), the mixed nature of the inhibition was confirmed. Both types of plots provide clear intersecting bundles of lines, as predicted for the case of mixed inhibition. From the median estimates of the direct plots a $K^*_{iu} = 534$ μM and a $K^*_{ic} = 377$ μM were determined as arsenite inhibitor constants for ArsC, in fairly good agreement with the values obtained with the full equation (Eq. 1) (Fig. 7).

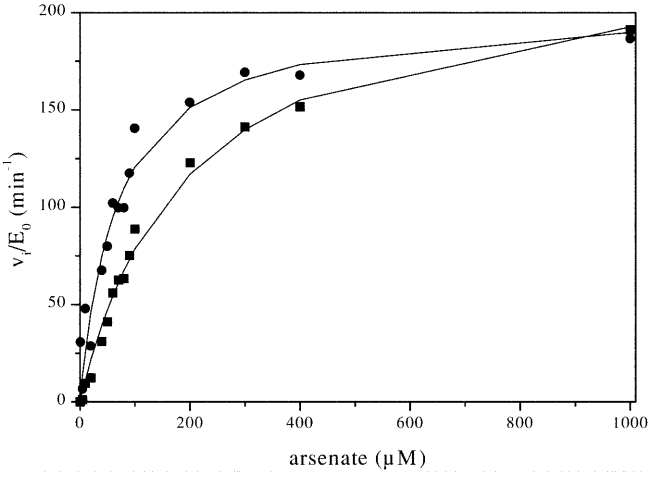

Fig. 6 Kinetic properties of ArsC wild-type and ArsC C15A. Michaelis-Menten kinetic plots of v_i/E_0 versus arsenate concentration of ArsC WT (*circles*) and ArsC C15A (*squares*)

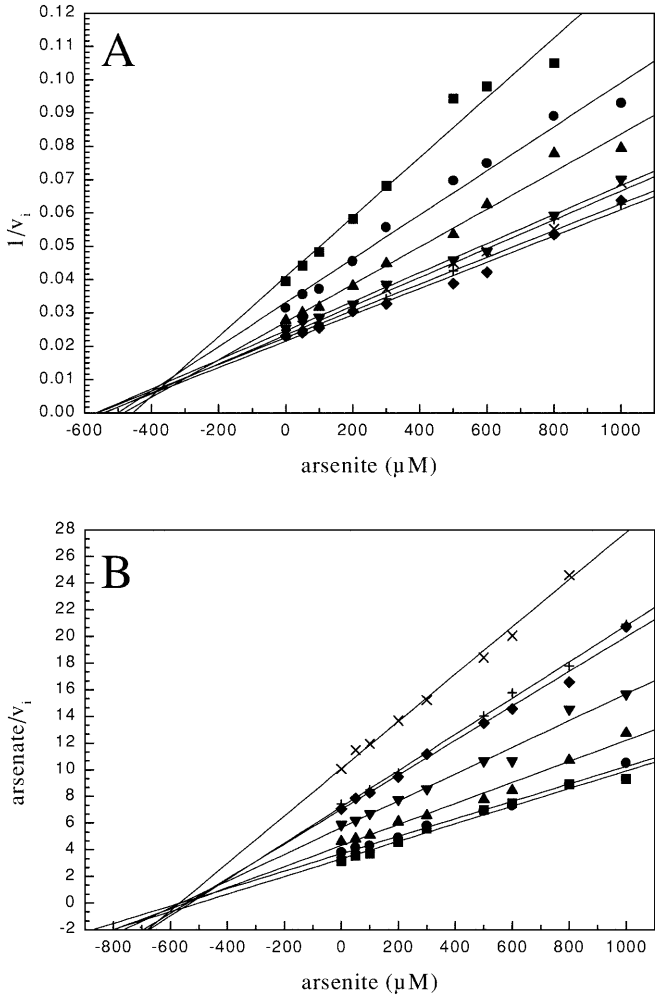

Fig. 7A, B Arsenite is a mixed inhibitor for ArsC. **A** $1/v_i$ plotted versus arsenite concentration at different arsenate concentrations: 80 μM (*squares*), 100 μM (*circles*), 125 μM (*triangles*), 150 μM (*reverse triangles*), 200 μM (*diamonds*), 250 μM (*vertical crosses*) and 300 μM (*diagonal crosses*). **B** Arsenate/v_i plotted versus arsenite concentration at different arsenate concentrations: 80 μM (*squares*), 150 μM (*circles*), 200 μM (*triangles*), 250 μM (*reverse triangles*), 300 μM (*diamonds*), 350 μM (*vertical crosses*) and 500 μM (*diagonal crosses*)

Antimonite and tellurite were also inhibiting the coupled reaction, as had been documented earlier. However, in the plot of v_i versus i, it was not possible to fit these data with a rectangular hyperbolic function. Here, inhibition was found to be substrate concentration independent. For tellurite an IC_{50} of 61 μM and for antimonite an IC_{50} of 32 μM were measured.

In an experiment where tellurite, antimonite and arsenite were preincubated for 5 min at 37 °C with the component mixture (Trx, TR and NADPH) from the cascade reaction and where oxidized ArsC was used as substrate, arsenite showed no inhibition. However, 100 μM tellurite and antimonite were found to inhibit the reaction. This leads us to conclude that only arsenite is a real arsenate reductase inhibitor, while tellurite and antimonite are inhibiting the reaction further down the cascade. None of them act as irreversible ArsC inactivator.

Discussion

In the absence of tetrahedral oxyanions it is impossible to correctly interpret the kinetic parameters, as the active ArsC concentration is steadily changing. The critical importance of keeping the concentration of the active form of this highly oxygen sensitive redox enzyme constant during the course of the enzymatic assay is shown. Often it is not noticed that enzymes lose activity, especially at low substrate concentrations. This results in a deviation of the initial rate from MM kinetics and can be falsely interpreted as cooperativity. A classic but often overlooked test to demonstrate whether the decrease in rate is due to enzyme inactivation, or not, is the Selwyn test. Here, it indicated that the presence of tetrahedral oxyanions (sulfate, phosphate, perchlorate or arsenate) is a strict requirement in order to obtain a single curve at different enzyme concentrations. Earlier studies (including our own) addressing the kinetic properties of ArsC never mentioned the absolute requirement of those stabilizing oxyanions in all assays, and as such, in the light of the current study, those data have to be taken within doubtful care. Previously, phosphate, arsenate and nitrate had been identified as activators, whereas for sulfate there was no sign or mention of an activity increase. We observed no increased rate of NADP production with nitrate and could clearly identify sulfate, phosphate, perchlorate and arsenate as stabilizing oxyanions (Fig. 4). In parallel, NMR spectroscopy of ^{15}N-labelled ArsC demonstrated that sulfate and arsenate (Fig. 5) bind to the Cys10-X_5-Arg16 segment and in doing so induce a more stable conformation of this loop. It is therefore not surprising that, under these structuring conditions, other kinetic data were measured than previously reported [10, 16]. The K_m (68 μM) measured in the presence of tetrahedral oxyanions (this report) are higher compared to the ones (66 nM, 1 μM) found in their absence [10, 16]. This confirms that for its reduction to arsenite, the arsenate substrate, itself a tetrahedral oxyanion, is binding at the same location in ArsC as do the stabilizing tetrahedral oxyanions. From the progress curves in Fig. 4, one may even conclude that arsenate is the optimal specific structuring agent among the tetrahedral oxyanions tested. The need for a high concentration of tetrahedral oxyanions to recover the NH correlations of these loop residues in NMR spectra indicates a modest affinity in the millimolar range, in perfect agreement with the appearance of the second step in the MM kinetics (Fig. 3).

The importance of oxyanions as agents, stabilizing the conformation, has also been documented for low molecular weight protein tyrosine phosphatases and for the *E. coli* ArsC from plasmid R773 [34, 35]. Using

NMR, phosphate and vanadate binding to the Cys12-X_5-Arg18-Ser19 tyrosine-phosphate-binding loop in PTPases was shown to be essential to observe residues Leu13 to Ser19 [34]. These residues align perfectly with residues Thr11 to Ser17 from ArsC, which are only visible in NMR spectroscopy when sulfate or arsenate binds. Using heteronuclear NMR spectroscopy, *E. coli* ArsC with an alternate H-X_3-C-X_3-R anion binding motif was characterized as "tending toward a dynamic extreme" [35]. In this case, binding of the substrate attenuated, but did not arrest the dynamics, with problematic consequences for a complete resonance assignment and high-resolution structure determination.

Previously [16], arsenite, tellurite and antimonite were identified as ArsC inhibitors and arsenate and selenate as substrates for ArsC. These results could not be confirmed under the optimized assay conditions. With this optimized enzymatic assay, we definitely observe substrate specificity for arsenate only. Also, the product of the arsenate reductase reaction, arsenite, was the only inhibitor of all oxyanions tested and was diagnosed as a mixed inhibitor. The simplest mechanistic interpretation for mixed inhibition is one in which the inhibitor (I) can bind both to the free enzyme (E) to give a complex EI with dissociation constant K_{ic}, as well as to the enzyme-substrate complex (ES) to give a complex ESI with dissociation constant K_{iu}. However, mixed inhibition occurs mainly as an important case of product inhibition. If a product (arsenite) is released in a step that generates an enzyme form (oxidized ArsC with a disulfide bridge between Cys82 and Cys89 [10]), different from the one to which the substrate binds (reduced ArsC), product inhibition is predicted to be in accordance with the equation defining mixed inhibition (Eq. 1) [29]. Both inhibition mechanisms can be considered for arsenite and might even act in concert. Under the optimized assay conditions where initial velocities were measured, product inhibition of arsenite is negligible, however, because the K_m for arsenate is more than five times lower ($K_m = 68$ μM) than the K_{ic} for arsenite ($K^*_{ic} = 377$ μM).

To the best of our knowledge, this report describes for the first time a redox enzyme that uses a substrate analogue (tetrahedral oxyanion) to structure its substrate (arsenate) binding-site in its active conformation. This is a peculiar observation, which was only possible with carefully purified and characterized enzyme. At present, it is not yet possible to link this observation to the in vivo environment of ArsC or to provide from these data more details about the complete reaction mechanism involved. The latter must await structural data of ArsC from *S. aureus* together with a kinetic analysis of mutants to determine the crucial residues in the vicinity of the active centre.

Acknowledgements We gratefully acknowledge Ingrid Zegers for thoughtful discussions and a critical review of the manuscript, Georges Laus for his professional help with mass spectrometry analysis and Dominique Maes for her mathematical advices and computer programming. We thank Simon Silver of the University of Illinois College of Medicine, Chicago, for the *arsC* gene of plasmid pI258, and Gerald Cohen and Orit Uziel of the Joan and Jaim Constantiner Institute for Molecular Genetics at the University of Tel-Aviv for the *trxA* and *trxB* genes of *S. aureus*. This work was funded in part by the VIB, Vlaams interuniversitair Instituut voor Biotechnologie. J.C.M. is a postdoctoral fellow of the Fund for Scientific Research Flanders (F.W.O.) (Belgium). R.W. and L.W. are indebted to the Fund for Scientific Research Flanders (F.W.O.) (Belgium), grant G.0192.98, and to the Research Council of the VUB (GOA6-1997-2001), for financial support.

References

1. Sanders OI, Rensing C, Kuroda M, Mitra B, Rosen BP (1997) J Bacteriol 179:3365–3367
2. Silver S, Keach D (1982) Proc Natl Acad Sci USA 79:6114–6118
3. Kuroda M, Bhattacharjee H, Rosen BP (1998) Methods Enzymol 292:82–97
4. Dey S, Dou D, Rosen BP (1994) J Biol Chem 269:25442–25446
5. Bröer S, Ji G, Bröer A, Silver S (1993) J Bacteriol 175:3840–3845
6. Chen C-M, Mobley HLT, Rosen BP (1985) J Bacteriol 161:758–763
7. Xu C, Zhou T, Kuroda M, Rosen BP (1998) J Biochem 123:16–23
8. Silver S, Ji G, Bröer S, Dey S, Dou D, Rosen BP (1993) Mol Microbiol 8:637–642
9. Ji G, Silver S (1992) J Bacteriol 174:3684–3694
10. Messens J, Hayburn G, Desmyter A, Laus G, Wyns L (1999) Biochemistry 38:16857–16865
11. Mukhopadhyay R, Shi J, Rosen BP (2000) J Biol Chem 275:21149–21157
12. Zhang Z-Y, Wang Y, Wu L, Fauman EB, Stuckey JA, Schubert HL, Saper MA, Dixon JE (1994) Biochemistry 33:15266–15270
13. Ramponi G, Stefani M (1997) Biochim Biophys Acta 1341:137–156
14. Zhang M, Stauffacher CV, Lin D, Van Etten RL (1998) J Biol Chem 273:21714–21720
15. Wang S, Tabernero L, Zhang M, Harms E, Van Etten RL, Stauffacher CV (2000) Biochemistry 39:1903–1914
16. Ji G, Garber EAE, Armes LG, Chen C-M, Fuchs JA, Silver S (1994) Biochemistry 33:7294–7299
17. Liu J, Rosen BP (1997) J Biol Chem 272:21084–21089
18. Messens J, Hayburn G, Brosens E, Laus G, Wyns L (2000) J Chromatogr B 737:167–178
19. Selwyn MJ (1965) Biochim Biophys Acta 105:193–195
20. Sambrook J, Fritsch EF, Maniatis T (1989) Molecular cloning: a laboratory manual, 2nd edn. Cold Spring Harbor Laboratory, Cold Spring Harbor, New York
21. Jacobs DM, Messens J, Brosens E, Wyns L, Wechselberger R, Willem R, Martins JC (2001) J Biomol NMR 21:95–96
22. Bodenhausen G, Ruben DJ (1980) Chem Phys Lett 69:185–189
23. Grzesiek S, Bax A (1993) J Am Chem Soc 115:12593–12594
24. Markley JL, Bax A, Arata Y, Hilbers CW, Kaptein R, Sykes BD, Wright PE, Wuthrich K (1998) Pure Appl Chem 70:117
25. Piotto M, Saudek V, Sklenar V (1992) J Biomol NMR 2:661–665
26. Marion D, Ikura M, Tschudin R, Bax A (1989) J Magn Reson 85:393–399
27. Laemmli UK (1970) Nature 227:680–685
28. Pace CN, Vajdos F, Fee L, Grimsley G, Gray T (1995) Protein Sci 4:2411–2423
29. Bunik V, Raddatz G, Lemaire S, Meyer Y, Jacquot JP, Bisswanger H (1999) Protein Sci. 8:65–74

30. Cornish-Bowden A (1995) Fundamentals of enzyme kinetics, rev. edn. Portland Press, London
31. Smith RM, Martell AE (1976) Critical stability constants, vol. 4. Plenum Press, New York
32. Dixon M (1953) Biochem J 55:170–171
33. Cornish-Bowden A (1974) Biochem J 137:143–144
34. Logan TM, Zhou MM, Nettesheim DG, Meadows RP, Van Etten RL, Fesik SW (1994) Biochemistry 33:11087–11096
35. Stevens SY, Hu W, Gladysheva T, Rosen BP, Zuiderweg ERP, Lee L (1999) Biochemistry 38:10178–10186